AN ALTERNATIVE POST-PROCESSING OF TRANSIENT LIQUID CRYSTAL EXPERIMENTS USING THE WALL TEMPERATURE GRADIENT TIME RESPONSE

Alexandros Peteinaris, Ohad Haftka, Alexandros Terzis
Thermo-Fluids & interfaces Lab
Faculty of Aerospace Engineering
Technion - Israel Institute of Technology
Haifa, 3200003, Israel

ABSTRACT

In this study, an alternative method for the fast evaluation of transient liquid crystal experiments is presented. The calibration of liquid crystals has been considered essential to obtain accurate heat transfer measurements. Nevertheless, liquid crystal aging, illumination, and ex situ calibration effects remain a difficult and might influence the heat transfer level. Proposed here is to bypass liquid crystal calibration, by utilizing the evolution of the wall temperature gradients. This necessitates the use of the detection times of the maximum red and green intensities of narrow bandwidth liquid crystals, e.g., less than 1 K, whose temperature span is on the order of 0.3 K. The calculation of the heat transfer coefficients can be thus feasible by differentiating the wall temperature from the solution of the semi-infinite body approach with respect to time. This approach was examined over different experiments with varying geometries and liquid crystal detection times. The possession of the calibration curves of the liquid crystals, in advance, allows for the cross-evaluation of the method. The results indicate that, despite local differences, the proposed method is in sufficiently good agreement with the values obtained using the calibrated liquid crystal signals. In particular, the average heat transfer coefficient of a surface is within 8% from the traditional method, which is sufficient for industrial applications and preliminary thermal designs.

NOMENCLATURE

c	Specific heat (J/kgK)
h	Heat transfer coefficient (W/m^{2}K)
k	Thermal conductivity (W/mK)
T	Temperature (°C)
t	Time (sec)

Greek symbols

ρ	Density (kg/m^3)

Subscripts

0	Initial conditions
avg	Average
g	Hot gas conditions
G	Green color signal
G-R	Difference of green and red color signals
LC	Liquid Crystal
R	Red color signal
w	wall

Abbreviations

HTC	Heat Transfer Coefficient
TLC	Thermochromic Liquid Crystal

INTRODUCTION

Advancements towards more effective thermal designs and efficient processes strongly relies on heat transfer phenomena, in various engineering applications. For their evaluation, the heat transfer coefficient is an informative indicator. Nevertheless, in convection transport processes, analytical and computational solutions are hard to get. To calculate the heat transfer coefficient, measuring techniques have been developed.

An established method incorporates the use of thermochromic liquid crystals [1]. The heat transfer coefficient of a surface subjected to a convective flow is calculated through the temperature evolution in the medium, which is described according to the semi-infinite body assumption. If lateral conduction phenomena are considered negligible, the solution of Fourier's 1-D conduction law provides the heat transfer coefficients as follows:

$$\frac{T_{LC}-T_0}{T_g-T_0} = 1 - \exp\left(\frac{h^2 t_{LC}}{\rho_w c_w k_w}\right) erfc\left(\frac{h\sqrt{t_{LC}}}{\sqrt{\rho_w c_w k_w}}\right) \quad (1)$$

where T_g is the temperature of the gas flow, T_0 is the initial surface temperature. T_{LC} and t_{LC} represent the optically monitored temperature of the liquid crystal and the detection time. ρ_w, c_w and k_w are the density, the specific heat and the thermal conductivity of the medium, respectively[2][3].

For the exploitation of the optical data of the camera numerous techniques have been deployed. A hue-based method, which was developed by Camci et al., correlates the color indication of the liquid crystals with temperature. They displayed that there is an effective range within the bandwidth of the liquid crystals, where the hue value increases linearly with temperature. In this way, an easier and time efficient observation of heat transfer processes on intricate surfaces has been enabled[4]. Although hue methods offer upsides, like the elimination of the background noise, they are useful primarily at steady state experiments[5]. Moreover, this method comes with high dependency of the linear region to

the lighting angle and the need to maintain identical camera settings both during the calibration process and the experiments[4].

A TLC indication based on the RGB color scheme through a peak intensity detection provides great upside at transient experiments. This method is particularly useful in experiments with complex geometries and phenomena in very small scales, or in applications with low light availability, as they display high sensitivity to weak signals[5]. The prevailing method is to utilize the peak intensity of the green color, as it is the most distinctive of the three colors[6][7] [8].

The aforementioned techniques have been the basis for the implementation of numerous methods. Wang et al., instead of applying a peak-intensity method, have utilized the entire intensity history to perform a more accurate measurement of the heat transfer coefficient.[9] On the other hand, Talib et al. used a combination of three different liquid crystals, while making multiple temperature steps to map the distribution of the heat transfer coefficients.[10] In this direction, Waidmann et al. used five different liquid crystals, in the range of 30 °C to 50 °C and demonstrated that the uncertainty in the calculation of the heat transfer coefficients based on multiple measurements can be of increased precision.[11] Alternatively, a multicolor technique for a single band TLC has been implemented. The suitability of the peak intensity of the red color for has been proven, since equally accurate measurements have been obtained[12]. Therefore, a double detection of the peak intensities of both the green and red colors allows for an even more precise measurement of temperature, without adding further complexity to the evaluation of the experimental data[13].

Calibration remains an inevitable step for the proper use of the liquid crystals. Abdullah et al. provide a thorough description of all the issues that inexperienced users may encounter as they attempt to perform calibration. Among others, for instance, setting up a suitable exposure system in the absence of white within the field of view and the effect of the film thickness is discussed.[14] In hue-temperature calibrations the derived color space highly depends on the white-light point, which does not necessarily lie in the reference hue point, thus necessitating an additional color calibration to avoid biased errors in the temperature measurement with the liquid crystals.[15] The film's thickness is highlighted, as an increasing thickness of the liquid crystal coating causes a swift in the peak green intensity, which now corresponds to a different temperature[16]. Whether heating or cooling experiments will be conducted, has to be specified beforehand, as well. The effect of hysteresis phenomena cannot be neglected because it is rather significant. Performing a calibration for the opposite process may result up to a 60% shift in the hue-temperature correspondence[17]. Finally, the aging of the liquid crystals is reviewed. As they undertake heating and cooling cycles the hue-temperature relationship is modified, inducing measurement errors[18]. Although more effects can be considered, like the surface preparation and the variation of the operating conditions, the complexity of an accurate calibration is evident.

In this study an alternative approach for a fast evaluation of transient liquid crystal experiments is presented. The calculation of the wall temperature gradient, according to the detection times of the red and peak intensities, utilizes an analytical expression for the direct determination of the heat transfer coefficients, without the precise knowledge of the temperature distribution on the surface.

CASE STUDIES

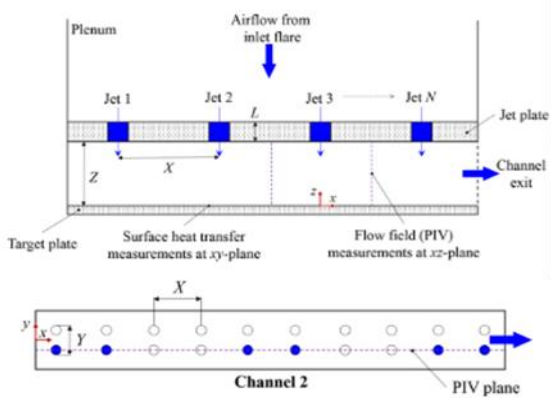

Figure 1: Front & Top view of the setup of the multiple jet impingement experiment [19]

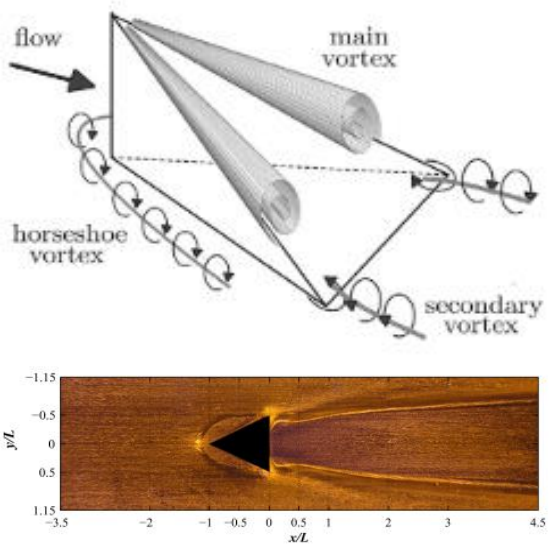

Figure 2: Schematic & Oil-flow visualization of a vortex generator [20]

In order to investigate the effectiveness of this alternative post-processing method, data from three different experiments are used. The first refers to a configuration of multiple jets impinging on a flat plate at high crossflow conditions[7] [21] [19]. The impingement channel, shown in Figure 1, consists of a double row of 10 jets impinging on a flat surface

while the spent air of the jets is forced to exit the channel in a single direction.

The second experiment examines the flow and heat transfer around a vortex generator of delta-wing shape design [20], as shown in Figure 2. In a similar configuration, the third experiment is related to a flow over a cylinder mounted on the flat plate.

METHODOLOGY

It has been assumed that the model surface can be approximated as a semi-infinite body, in which the temperature is described in Eqn. 1. Instead of using calibrated liquid crystals to directly acquire the temperature field, Eqn. 1 is differentiated to form an expression for the temperature gradient as a function of time, it is derived:

$$T = T_0 + (T_g - T_0)\left[1 - \exp\left(\frac{h^2 t_{LC}}{\rho_w c_w k_w}\right)\mathrm{erfc}\left(\frac{h\sqrt{t_{LC}}}{\sqrt{\rho_w c_w k_w}}\right)\right] \Rightarrow$$

$$\Rightarrow \frac{\partial T}{\partial t} = (T_g - T_0)\left[\frac{h}{\sqrt{b\pi t}} - \frac{h^2}{b}\exp\left(\frac{h^2 t}{b}\right)\mathrm{erfc}\left(\frac{h\sqrt{t}}{b}\right)\right] \quad (2)$$

where $b = \sqrt{\rho_w c_w k_w}$ incorporates material constants.

At this stage, the determination of the heat transfer coefficient in a single point depends on the calculation of the wall temperature gradient and the determination of time. Even for a single value of the temperature gradient, there are infinite solutions to Eqn. 2, as different pairs of (h, t) satisfy the equality.

The first step towards the calculation of the heat transfer coefficient is the determination of the wall temperature gradient. By applying a first-order finite expression, the gradient is selected to be the ratio of the temperature difference of green and red at their peak intensities to the time difference between the detection times of liquid crystals, as follows:

$$\frac{\partial T}{\partial t} = \frac{\Delta \mathrm{T_{G-R}}}{\Delta t_{\mathrm{G-R}}} = \frac{T_G - T_R}{t_G - t_R} \quad (3)$$

The time steps t_G, t_R are directly obtained by the video data. However, of the determination of the temperature difference, the knowledge of the calibration curves is demanded.

Instead of resolving the issues rising from the difficult and time-intensive calibration of the liquid crystals, it is selected to bypass it. This decision finds preferable application in narrowband liquid crystals, which are of higher accuracy that wide-band TLCs. The review of the relative literature is summarized in Table 1, where the temperatures corresponding to the maximum intensity of the red and green color are listed. According to them, it is shown that, in narrowband liquid crystals with an effective range of approximately 1 °C, a typical temperature difference $\Delta T_{G\text{-}R}$ varies between 0.2 °C and 0.4 °C. Consequently, it is reasonable to assume a value within this temperature range.

Table 1: Temperature data on the maximum intensity of reg and green colors

Experiment	T_R [°C]	T_G [°C]	$\Delta T_{G\text{-}R}$ [°C]
R30C1W - 30 μm [18]	31.1	31.4	0.3
R30C1W - 45 μm [18]	31.0	31.3	0.3
R35C1W - Heating[17]	35.9	36.1	0.2
R35C1W -Cooling[17]	35.8	36.1	0.3
SPN100G35C1W[13]	34.4	34.7	0.3
R38C1W[7]	38.1	38.5	0.4
R36C1[20]	36.45	36.7	0.25

Hereupon, it is necessary to treat the image data of the camera. Part of the procedure, as described by Poser et al. is followed[3]. First of all, temporal filter for noise reduction is applied. Wavelet functions allow for the inclusion of both high- and low-frequency signals in the output. Furthermore, they are more appropriate for TLC experiments due to the discontinuities and aperiodic signals with abrupt fluctuations, that are produced by the liquid crystals. Thus, the calculation of the approximated wall temperature gradient is possible.

Finally, towards the calculation of the heat transfer coefficient, demands the proper solution of the Eqn. 2., which has infinite solutions. Therefore, the selection of the correct pair (h, t) is critical. Figure 3 shows that for a given wall temperature gradient, Eqn. 2 has up to 2 solutions. Because the unknown variables (h, t) exceed the available equations, throughout the study it is assumed that the values of the wall temperature gradients are obtained in the medial time between the two intensity peaks of the red and green signals. Under these conditions, both solutions of Eqn 2., as shown in Figure 3, may be plausible. Therefore, the consideration of both solutions not only separately, but also combined, to account for inaccuracies in the time selection, are proposed.

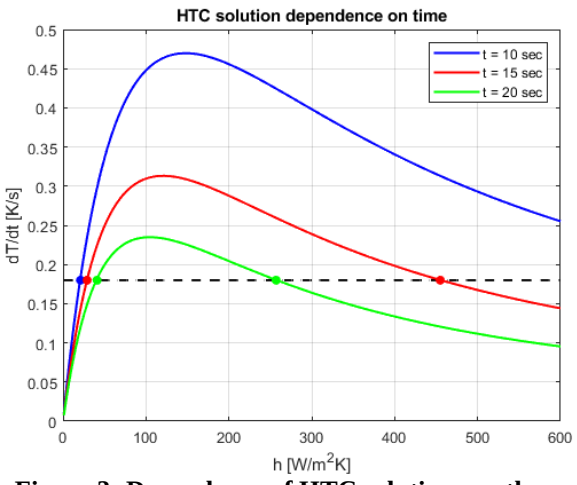

Figure 3: Dependence of HTC solutions on the selection of time

RESULTS

Figure 4 illustrate the spatial distribution of the wall temperature gradients for all case studies. The accuracy of the proposed post-processing technique can be evaluated by directly comparing it with the distributions according to the red- and green-color signals of the calibrated liquid crystals.

Figure 4a is related to the experiment of a flow around a cylinder. Although the distributions of the temperature wall gradients, according to the red- and green-color signals, look very similar, differences can be observed locally. The red-color scheme leads to slightly higher temperature wall gradients. This is evident particularly in the leading edge of the plate and downstream the cylinder, in the flow, where extended regions of higher gradients are provided.

For uncalibrated liquid crystals, as expected, the proposed method leads to a distorted temperature gradient field on the plate surface. In the leading edge, the gradients' field resembles more the red-color signal, because of the higher gradients that are calculated for a prolonged region. The high-gradient region around the cylinder is well-approximated, too. However, differences are observed downstream the cylinder. Locally, the gradient approximation lacks of accuracy in determining the gradient values. The pixel resolution is more pronounced, because the transition from lower to higher gradients' regions is not smooth. High and low temperature-gradient pixels are alternating in neighboring positions.

In the experiment with the flow around a vortex generator, similar results are obtained. The red- and green-color signal distributions are almost identical. The differences between the alternative approach and the others of the calibrated liquid crystals are identified at the region of the stagnation point in front of the vortex generator and downstream, at its wake. The two-color method overestimates the temperature gradients in the stagnation point, while it underestimates the respective values around the vortex generator. More, particularly, on its back side, the high temperature gradients section with values higher than 0.3 K/s is limited to a smaller area.

Finally, Figure 4c illustrates the differences of the investigated techniques in the experiment of the multiple jets' impingement. The depictions of the temperature wall gradient field on the plate of the red- and green-color signals demonstrate a smooth transition from the lower to the highest values. The peaks are observed in the regions, where the jets impinge. Compared to the green-color, the red-color scheme leads to extended regions of gradients higher than 1.5 K/s in the locations of the impingement.

The alternative method, which is shown in the middle picture, is not able to accurately calculate the gradients at the impingement locations, leading to a

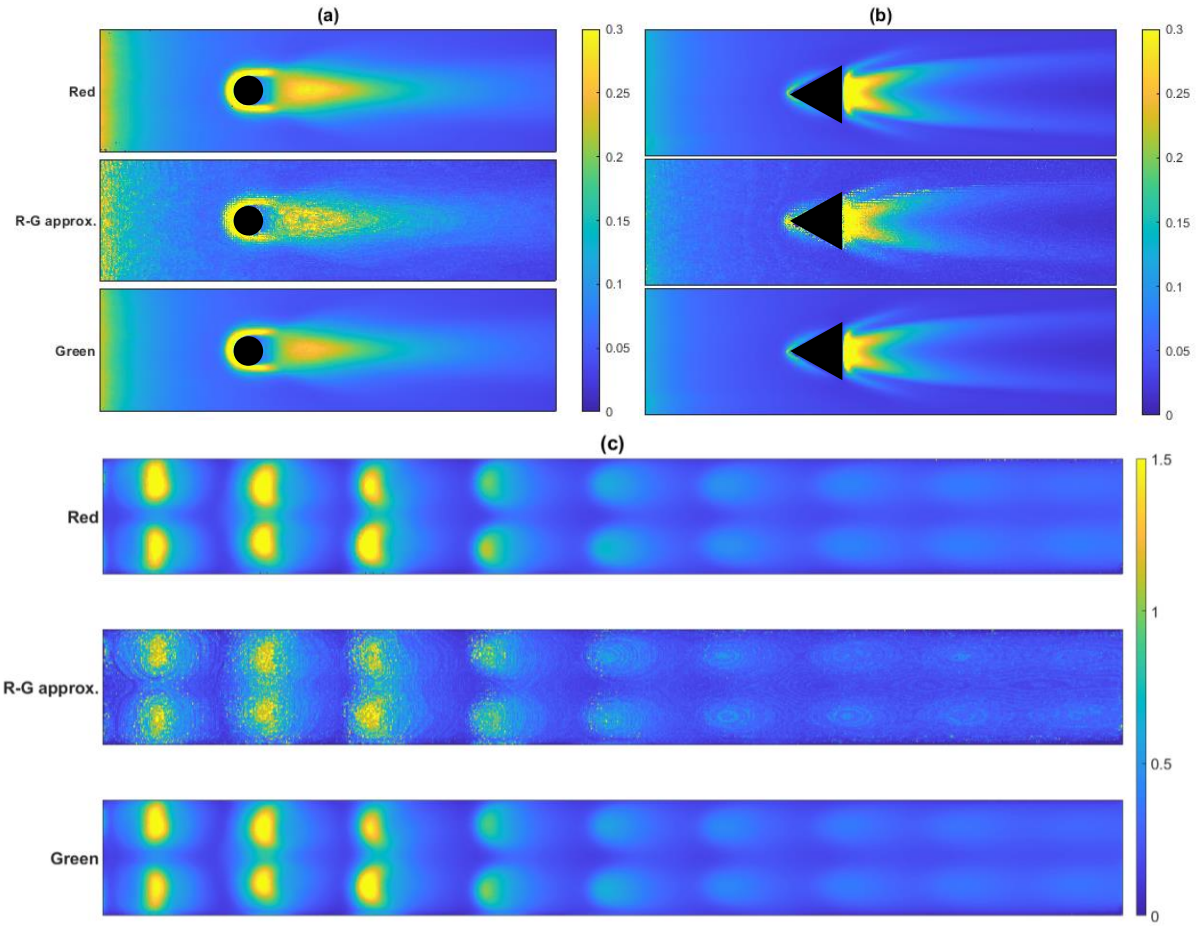

Figure 4: Wall temperature gradient distribution for (a) the cylinder (b) vortex generator & (c) multiple impingement jets experiments according to red and green signals and the R-G approximation

field with substantially lower values in the region of the first impinging jets. Moreover, this trend further extends downstream the plate. Even the jets, which are almost totally deflected, where the temperature gradients are lower, this approach leads to slightly lower values. The approximation of the gradients is not spatially coherent, as well, since the temperature gradients are fluctuating in successive pixels.

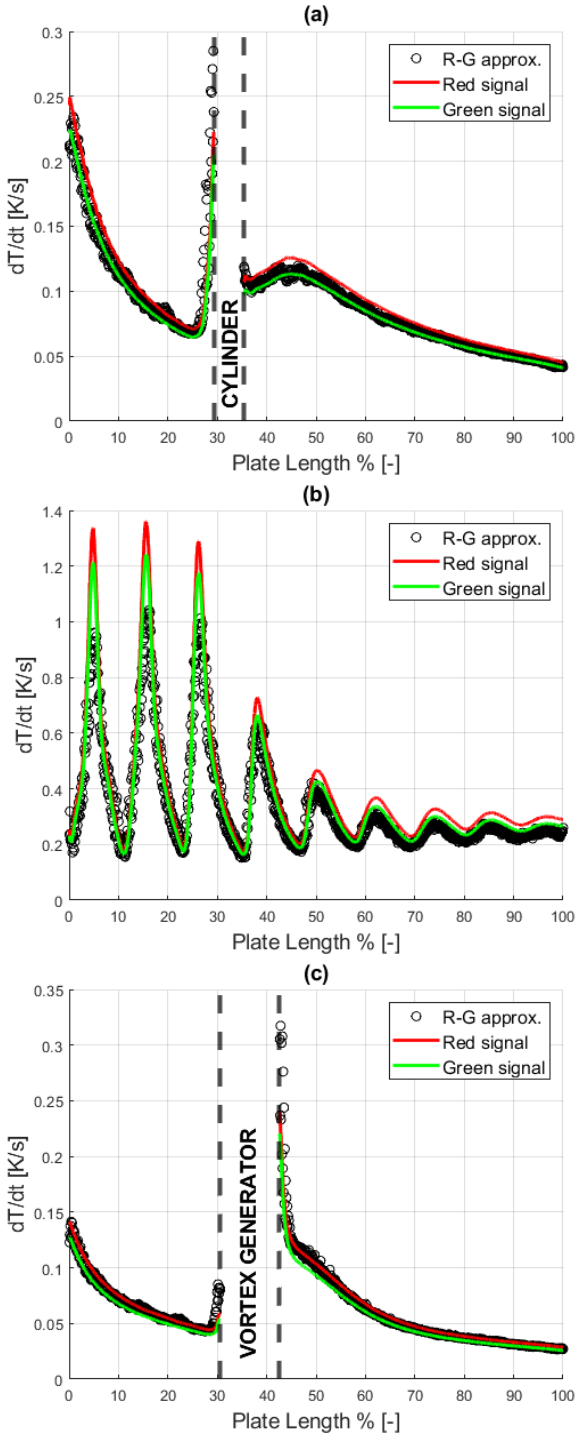

Figure 5: Spanwise average of wall temperature gradients for (a) the cylinder, (b) multiple impingement jets and (c) vortex generator experiment

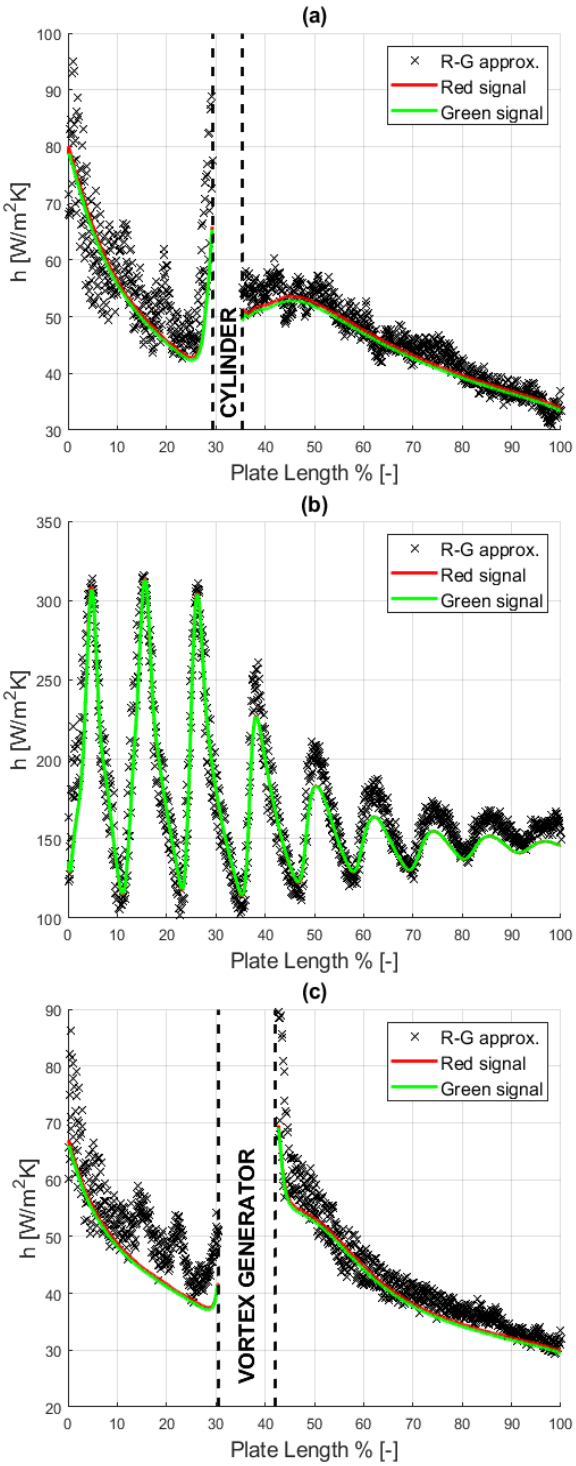

Figure 6: Spanwise average of HTC for (a) the cylinder, (b) multiple impingement jets and (c) vortex generator experiment

Nevertheless, if an averaging of the gradients is applied spanwise, as it is presented in Figure 5, the results are in good agreement. Either in case of the flow around a cylinder or a vortex generator, the spanwise averaged temperature wall gradients are coincident with the results from the calibrated liquid crystals in the regions away from the geometry. However, as it was shown in Figure 4, the alternative

approach miscalculates the gradients close to the solid body. At the stagnation point of the cylinder the temperature gradient is overestimated and the same effect is observed right after the vortex generator.

Finally, in the multiple jets' impingement case, the spanwise averaged temperature gradients of the alternative approach are constantly lower compared to the standard methods. The trend is highlighted not only in the impingement location of the first jets, but also in the region of the highly deflected jets. This deviation could be justified by the inaccuracy in the estimation of the temperature difference between red and green maximum intensities.

In Figure 6 the evolution of the averaged heat transfer coefficient is illustrated. The proposed post-processing method results in higher heat transfer coefficients across the length of the plate for all of the studied cases, compared to the standard methods with the use of the calibrated liquid crystals.

The provided solutions for the experiments of the cylinder and the vortex generator also display higher discrepancy in the calculated heat transfer coefficient values. In these cases, at each pixel the lower heat transfer coefficient solution was selected as the most suitable, due to the very low temperature gradients of the field. On the other side, in the multi-jet impingement experiment, the alternative method provides results with noticeably reduced variance. Furthermore, the results match the heat transfer coefficients of the calibrated liquid crystals. However, downstream in the latter jets' locations, the heat transfer coefficient is overestimated. This change in the accuracy of the solutions along the plate could be attributed to the selection process of the solutions. As very high heat transfer coefficients are expected in the region of the first jets, an averaging of the two probable solutions is considered the optimal approach. Nevertheless, as the heat transfer coefficient reduces along the plate, the accuracy of this approach reduces, as well.

The averaging of the heat transfer coefficient fields according to the various presented methods for the three investigated experiments reveals the accuracy of the proposed technique. In Table 2 the area-averaged results on the HTC are summarized. In the last column the average deviation of the presented approach from the red- and green-signal method is shown.

Table 2: Comparison of the area-averaged HTCs

Experiment	$\bar{\bar{h}}_R$	$\bar{\bar{h}}_G$	$\bar{\bar{h}}_{G-R}$	Δh_{avg}
Cylinder	44.7	47.1	49.1	7 %
Impingement Jets	165.7	166	172.5	4 %
Vortex Generator	42.7	42.2	45.8	7.9 %

It is indicated that, despite the rough estimation of the temperature difference between the red and green maximum intensity, this alternative method can be sufficiently accurate. The additional error in the determination of the heat transfer coefficient hardly exceeds 8%, in the experiment with the vortex generator, while in the respective experiment of the flow around the cylinder, it is less than 4%.

UNCERTAINTY ANALYSIS

To estimate the experimental uncertainties that rise throughout the calculation procedure of this alternative post-processing approach, the method of small perturbations can be applied.[22][23]

The analysis is applied in two steps. First of all, the uncertainty in the estimation of the temperature gradient is calculated. Subsequently, the same procedure is repeated for the calculation of the HTC. For an experiment with N independent variables X_i, the uncertainty is derived with the root-sum-squared method, as shown in Eqn. 4 and Eqn. 5 below:

$$\delta\left(\frac{\partial T}{\partial t}\right) = \sqrt{\sum_{i=1}^{N}\left(\frac{\partial \frac{\partial T}{\partial t}}{\partial X_i}\right)^2 P_{X_i}^2} \tag{4}$$

$$\delta h = \sqrt{\sum_{i=1}^{N}\left(\frac{\partial h}{\partial X_i}\right)^2 P_{X_i}^2} \tag{5}$$

Table 3: Uncertainties in the temperature gradient approximation

Parameter	Units	Value	Error	$\Delta\left(\frac{\partial T}{\partial t}\right)$ %
ΔT_{G-R}	(°C)	0.3	±0.1	31
Δt_{avg}	(sec)	1.17	±0.15	4.6
$\left(\frac{\partial T}{\partial t}\right)_{avg}$	(K/s)	0.256		~35.7

The calculation of the wall temperature gradient is dependent on the estimation of the temperature difference between the red and green maximum intensities and their timestep of occurrence and the observation of times of the peak color intensities. The results, as they are presented in Table 3, reveal the predominant role of the guess of the temperature difference in the error propagation of the estimation of the temperature wall gradient.

For the uncertainty in the calculation of the heat transfer coefficient, the calculations were performed in 3 separate timesteps t_i. Table 4 summarizes the parameter values that were used.

Despite the large uncertainty in the estimation of the wall temperature gradient, its contribution in the uncertainty of the heart transfer coefficient is low. The time t_i is the primary source of uncertainty, as it is shown in Table 5. For increasing time t_i and decreasing HTC, the uncertainty increases up to 28.3%, as the contribution of time and gradient grow larger. The calculation of the HTC is influenced by

the temperature conditions of the experiment and the thermal properties of the plate, too. Nevertheless, their effect is relatively negligible, since it does not surpass 0.5%.

Table 4: Value selection for the uncertainty analysis

Parameter	Units	Value	Error
T_0	(°C)	18.5	±0.1
T_g	(°C)	52.4	±0.1
$\sqrt{\rho_w c_w k_w}$	$W\sqrt{s}/m^2K$	569	±28.5
$\left(\frac{\partial T}{\partial t}\right)_{avg}$	(K/s)	0.256	±0.09
t_1	(sec)	10	±0.15
h_1	(W/m^{2}K)	314.5	
t_2	(sec)	12.5	±0.15
h_2	(W/m^{2}K)	217.5	
t_3	(sec)	15	±0.15
h_3	(W/m^{2}K)	158.5	

Table 5: Parameters' contribution in the heat transfer coefficient uncertainty

$P_{X,i}$	Δh% @h_1	Δh% @h_2	Δh% @h_3
P_t	14	14.9	19.6
$P_{\frac{\Delta T}{\Delta t}}$	1.2	2.9	8.2
P_b	0.4	0.3	0.2
P_{T_g}	0.05	0.1	0.2
P_{T_o}	0.02	0.04	0.1
P_h	15.67	18.24	28.3

CONCLUSIONS

This study presented an alternative technique for the post-processing of the results of transient experiments with the use of liquid crystals. The aim has been to produce a technique that allows for the faster execution of liquid crystal experiments and evaluation of their results. To achieve that, the time-consuming and highly sensitive calibration process is omitted. With an emphasis on narrowband liquid crystals, it has been proposed to calculate the heat transfer coefficient through the estimation of the temporal evolution of the wall temperature gradient, under the assumption of a semi-infinite body. Thus, the temperature difference between the maximum intensities of the red- and green-color signals has been arbitrarily selected. This technique was tested for three separate experimental cases. Following the application of this alternative method, an uncertainty analysis was carried out to identify the influence of the related parameters.

The results revealed that over the entire surface, the estimation of the wall temperature gradient is sufficiently accurate. Nevertheless, distinguishing over- or underestimations were observed, which are attributed to the low accuracy of the finite difference expression that was used for the calculation. Despite these local effects, a spanwise averaging has shown that this alternative technique agrees with the results of calibrated liquid crystals, particularly when the time constant of heat transfer is low.

The appropriate selection of the solutions of the temperature gradient equation enables the accurate determination of the heat transfer coefficient. It was proven that, despite the inability to know the actual temperature difference of the colors, this technique can be accurate. The produced deviation between the techniques, which does not exceed 8% highlights the utility of this alternative post-processing technique, particularly in industrial applications.

REFERENCES

[1] P. T. Ireland and T. V. Jones, "Liquid crystal measurements of heat transfer and surface shear stress," *Meas. Sci. Technol.*, vol. 11, no. 7, pp. 969–986, 2000, doi: 10.1088/0957-0233/11/7/313.

[2] A. Terzis, S. Bontitsopoulos, P. Ott, J. Von Wolfersdorf, and A. I. Kalfas, "Improved accuracy in jet impingement heat transfer experiments considering the layer thicknesses of a triple thermochromic liquid crystal coating," *J. Turbomach.*, vol. 138, no. 2, pp. 1–10, 2016, doi: 10.1115/1.4031786.

[3] R. Poser and J. von Wolfersdorf, "Transient liquid crystal thermography in complex internal cooling systems."

[4] C. Camci, K. Kim, and S. A. Hippensteele, "A new hue capturing technique for the quantitative interpretation of liquid crystal images used in convective heat transfer studies," *J. Turbomach.*, vol. 114, no. 4, pp. 765–775, 1992, doi: 10.1115/1.2928030.

[5] R. Poser, J. von Wolfersdorf, and E. Lutum, "Advanced evaluation of transient heat transfer experiments using thermochromic liquid crystals," *Proc. Inst. Mech. Eng. Part A J. Power Energy*, vol. 221, no. 6, pp. 793–801, 2007, doi: 10.1243/09576509JPE464.

[6] L. V. Tran and C. D. Slabaugh, "On correlated measurements in the transient thermochromic liquid crystals technique with multiple indicators," *Int. J. Heat Mass Transf.*, vol. 137, pp. 229–241, 2019, doi: 10.1016/j.ijheatmasstransfer.2019.03.077.

[7] S. L. Sanllehí, "Experimental evaluation of local heat transfer distributions in high crossflow narrow impingement channels using the transient liquid crystal technique," Ecole Polytechnique Federale de Lausanne, 2014.

[8] A. Terzis, "Detailed heat transfer distributions of narrow impingement channels for cast-in turbine airfoils," ÉCOLE POLYTECHNIQUE FÉDÉRALE

DE LAUSANNE, 2014. doi: 10.1115/1.4027679.

[9] Z. Wang, P. T. Ireland, and T. V. Jones, "An advanced method of processing liquid crystal video signals from transient heat transfer experiments," *ASME 1993 Int. Gas Turbine Aeroengine Congr. Expo. GT 1993*, vol. 3B, no. January, 1993, doi: 10.1115/93-GT-282.

[10] A. R. A. Talib, A. J. Neely, P. T. Ireland, and A. A. J. Mullender, "A novel liquid crystal image processing technique using multiple gas temperature steps to determine heat transfer coefficient distribution and adiabatic wall temperature," *J. Turbomach.*, vol. 126, no. 4, pp. 587–596, 2004, doi: 10.1115/1.1776585.

[11] C. Waidmann, R. Poser, and J. Von Wolfersdorf, "Application of thermochromic liquid crystal mixtures for transient heat transfer measurements," *10th Eur. Conf. Turbomach. Fluid Dyn. Thermodyn. ETC 2013*, pp. 685–696, 2014.

[12] J. S. K. Lucky V. Tran, Anne L. Pham, Zachary D. Little, "Characterization of Thermochromic Liquid Crystals for Multi-Color Transient Heat Transfer Experiments," pp. 1–7, 2013, doi: 10.2514/6.2013-3012.

[13] L. V. Tran, A. L. Pham, Z. D. Little, and J. S. Kapat, "A multi-color thermochromic liquid crystals technique for transient heat transfer experiments," *44th AIAA Thermophys. Conf.*, pp. 1–10, 2013, doi: 10.2514/6.2013-3013.

[14] N. Abdullah, A. R. Abu Talib, A. A. Jaafar, M. A. Mohd Salleh, and W. T. Chong, "The basics and issues of Thermochromic Liquid Crystal Calibrations," *Exp. Therm. Fluid Sci.*, vol. 34, no. 8, pp. 1089–1121, 2010, doi: 10.1016/j.expthermflusci.2010.03.011.

[15] J. H. Sun, K. C. Leong, and C. Y. Liu, "Influence of hue origin on the hue-temperature calibration of thermochromic liquid crystals," *Heat Mass Transf. und Stoffuebertragung*, vol. 33, no. 1–2, pp. 121–127, 1997, doi: 10.1007/s002310050168.

[16] N. Abdullah, A. R. Abu Talib, H. R. Mohd Saiah, A. A. Jaafar, and M. A. Mohd Salleh, "Film thickness effects on calibrations of a narrowband thermochromic liquid crystal," *Exp. Therm. Fluid Sci.*, vol. 33, no. 4, pp. 561–578, 2009, doi: 10.1016/j.expthermflusci.2008.12.002.

[17] M. R. Anderson and J. W. Baughn, "Hysteresis in liquid crystal thermography," *J. Heat Transfer*, vol. 126, no. 3, pp. 339–346, 2004, doi: 10.1115/1.1738425.

[18] V. U. Kakade, G. D. Lock, M. Wilson, J. M. Owen, and J. E. Mayhew, "Accurate heat transfer measurements using thermochromic liquid crystal. Part 1: Calibration and characteristics of crystals," *Int. J. Heat Fluid Flow*, vol. 30, no. 5, pp. 939–949, 2009, doi: 10.1016/j.ijheatfluidflow.2009.04.007.

[19] A. Terzis, "On the correspondence between flow structures and convective heat transfer augmentation for multiple jet impingement," *Exp. Fluids*, vol. 57, no. 9, pp. 1–14, 2016, doi: 10.1007/s00348-016-2232-7.

[20] A. Terzis, J. von Wolfersdorf, B. Weigand, and P. Ott, "A method to visualise near wall fluid flow patterns using locally resolved heat transfer experiments," *Exp. Therm. Fluid Sci.*, vol. 60, pp. 223–230, 2015, doi: 10.1016/j.expthermflusci.2014.09.009.

[21] A. Terzis, J. Von Wolfersdorf, B. Weigand, and P. Ott, "Thermocouple thermal inertia effects on impingement heat transfer experiments using the transient liquid crystal technique," *Meas. Sci. Technol.*, vol. 23, no. 11, 2012, doi: 10.1088/0957-0233/23/11/115303.

[22] R. J. Moffat, "Describing the uncertainties in experimental results," *Exp. Therm. Fluid Sci.*, vol. 1, no. 1, pp. 3–17, 1988, doi: 10.1016/0894-1777(88)90043-X.

[23] Y. Yan and J. M. Owen, "Uncertainties in transient heat transfer measurements with liquid crystal," *Int. J. Heat Fluid Flow*, vol. 23, no. 1, pp. 29–35, 2002, doi: 10.1016/S0142-727X(01)00125-4.